Anal. Chem. **1999,** *71,* 1176−1182

Effects of Chloride Ion Concentration on Mercury(I) Chloride Formation during ex Situ and in Situ Mercury Deposition with Selected Electrode Substrates and Electrolytes

Melissa A. Nolan and Samuel P. Kounaves*

Department of Chemistry, Tufts University, Medford, Massachusetts 02155

Ex situ and in situ mercury film formation was investigated in solutions containing NO_3^-, SCN^-, Cl^-, and ClO_4^-, and at glassy carbon macro- (3 mm) and micro- (10 μm) electrodes, a platinum macro- (1.6 mm) electrode, and a microfabricated Ir-ultramicroelectrode array (Ir-UMEA). The formation of mercury(I) chloride (calomel) during Hg deposition was investigated by varying the Cl^- concentration. The performance of the Hg films was evaluated using Cd^{2+} and Pb^{2+} with square wave anodic stripping voltammetry. For ex situ Hg film formation on Ir and GC substrates, the highest efficiency was obtained when no Cl^- or 1 M Cl^- was present. The Pt surface was affected by the Cl^- ions; thus for ex situ Hg film formation, the best results were obtained with no Cl^- present. Calomel formation during in situ Hg deposition occurred for $0.001 > [Cl^-] < 0.5$ M and was independent of the substrate. Calomel interference was identified by the presence of an anomalous cathodic peak between −0.6 and −0.3 V during the anodic scan. For in situ Hg film formation, the Pb^{2+} stripping peak current increased with increasing ionic strength, while the Cd^{2+} peak current increased dramatically in the presence of SCN^- or Cl^-. Although conditioning of the Ir-UMEA and Pt macroelectrode eliminated the cathodic peak, calomel still remained on the surface after the Hg film was removed. When the cathodic peak was present, no calomel remained after removal of the Hg film; thus for in situ film formation, the calomel interference can be avoided. When $[Cl^-] > 0.01$ M, the best results can be obtained by adjusting $[Cl^-]$ to 1 M. For $[Cl^-] < 0.01$ M, addition of SCN^- is recommended. Although analyses can be preformed without any Cl^- present, precautions should be taken to avoid unintentional contamination.

In anodic stripping voltammetry (ASV), mercury is still the electrode of choice for heavy metal analysis. The mercury film electrode (MFE) has been increasingly used in preference to the hanging mercury drop electrode (HMDE) because it offers higher sensitivity, more efficient preconcentration, sharper peaks, and improved peak resolution for multicomponent analysis.[1] The most common substrate used for mercury film formation is glassy carbon because, unlike metal substrates such as gold and platinum, it is inert to mercury. Iridium has also been shown to be an excellent substrate for mercury film formation [2−4] because of its low solubility in mercury (below 10^{-6} wt %) and good wettability.[5,6]

In situ deposition of mercury films on glassy carbon substrates has been demonstrated as an acceptable procedure for mercury film formation.[7−15] There are several advantages to forming an in situ mercury film: (1) a decrease in analysis time because the requirement for a separate deposition procedure is eliminated, (2) possibility of damaging the film substantially reduced since the mercury electrode does not have to be transferred between different solutions, (3) a decrease in the possibility of cross contamination, and (4) the automatic generation of a new mercury surface for every analysis. In several previous studies,[8,10−12,15] it was recognized that chloride ions interfere with the in situ deposition of mercury films due to the formation of insoluble calomel (Hg_2Cl_2) on the mercury surface. The formation of calomel on the electrode surface during the anodic scan results in an anomalous cathodic peak as shown in Figure 1. The cathodic peak distorts and interferes with analyte stripping peaks between −0.6 and −0.3 V. Also, the presence of calomel leads to an undefined electrode surface morphology which could effect all analyte responses. There are currently two methods for avoiding the calomel interference, either by addition of KSCN to the mercury solution[10] or by using a chloride concentration of greater than 3.5 M.[15]

* Corresponding author.

(1) Wang, J. *Analytical Electrochemistry*; VCH Publishers: New York, 1994.
(2) Kounaves, S.; Buffle, J. *J. Electroanal. Chem.* **1988**, *239*, 113−123.
(3) Kounaves, S.; Deng, W. *Anal. Chem.* **1993**, *65*, 375−379.
(4) Tercier, M.-L.; Parthasarathy, N.; Buffle, J. *Electroanalysis* **1995**, *7*, 55−63.
(5) Guminski, C.; Galus, Z. *Solubility Data Series−Metals in Mercury*; Pergamon Press: Oxford, UK, 1986.
(6) Kounaves, S. P.; Buffle, J. *J. Electrochem. Soc.* **1986**, *133*, 2495.
(7) Florence, T. M. *J. Electroanal. Chem.* **1970**, *27*, 273.
(8) Wu, H. P. *Anal. Chem.* **1994**, *66*, 3151−3157.
(9) Wu, H. P. *Anal. Chem.* **1996**, *68*, 1639−1645.
(10) Wojciechowski, M.; Balcerzak, J. *Anal. Chim. Acta* **1991**, *249*, 433−445.
(11) Wojciechowski, M.; Balcerzak, J. *Anal. Chem.* **1990**, *62*, 1325−1331.
(12) Frenzel, W. *Anal. Chim. Acta* **1993**, *273*, 123−127.
(13) Komorsky-Lovric, S.; Lovric, M.; Bond, A.M. *Anal. Chim. Acta* **1992**, *258*, 299−305.
(14) Baranski, A. S. *Anal. Chem.* **1987**, *59*, 662−666.
(15) Jagner, D.; Sahlin, E.; Renman, L. *Anal. Chem.* **1996**, *68*, 1616−1622.

10.1021/ac9808270 CCC: $18.00
Published on Web 02/06/1999

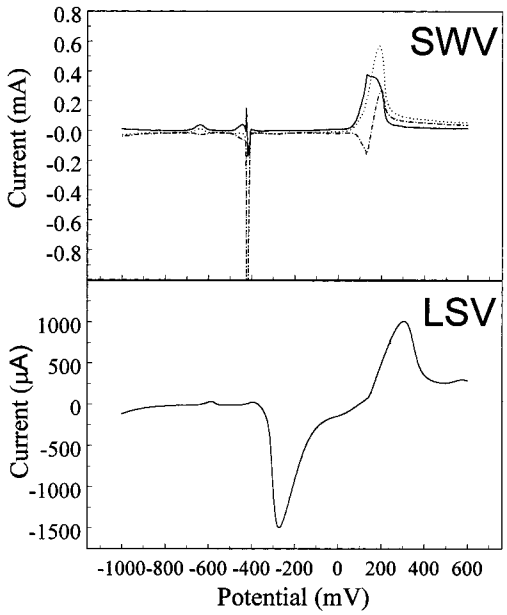

Figure 1. Forward (●), reverse (– · –), and net current (—) response for SWV with $f = 60$ Hz, $E_{sw} = 25$ mV, and $\Delta E_s = 2$ mV and for single-scan LSV with $\nu = 500$ mV/s, both with a solution containing 0.8 mM Hg^{2+}, 0.01 M HNO_3, and 0.1 M NaCl and using a macro-GCE as working electrode.

Previous studies of in situ mercury deposition have been performed on glassy carbon electrodes mainly because of its high hydrogen overpotential. Other metal substrates such as platinum and iridium have lower hydrogen overpotentials, and thus the deposition of the mercury and the analyte metals can rarely be performed simultaneously. However, a mercury deposition performed in two steps is one way to circumvent this problem. Although not a typical in situ deposition, since the deposition of mercury and the analyte metals occur sequentially, it still occurs in the same solution. In the first step, mercury is deposited onto the electrode and then, in the second step, the analyte metals are deposited at a more negative potential simultaneously with more mercury. It is critical that enough mercury is deposited in the first step so that the electrode acts as a mercury electrode for the second step. Although this procedure increases analysis time, it still has all the other advantages described above.

In this study, the effect of chloride concentration on ex situ and in situ plated mercury films was investigated. Glassy carbon, platinum, and iridium were used as substrates for mercury film formation. The main goals were to determine the following: the chloride concentration at which calomel interferes, the best way to avoid calomel interference, and the role of the electrode substrate in calomel formation.

EXPERIMENTAL SECTION

Apparatus. Chronoamperometry, controlled-potential coulometry, linear scan voltammetry (LSV), differential pulse voltammetry (DPV), and square wave anodic stripping voltammetry (SWASV) experiments were performed with an EG&G PAR model 273 potentiostat/galvanostat (EG&G PAR, Princeton, NJ) interfaced to a DEC p420-SX microcomputer using model 270 software (EG&G PAR). All voltammetric experiments were performed in a three-electrode cell consisting of the working electrode, reference electrode, and a Pt wire counter electrode. Two different reference electrodes were used. For solutions with a chloride concentration greater than 1 M, a Ag/AgCl (3 M NaCl) reference electrode (BAS, West Lafayette, IN) was used. For all other solutions, a polyurethane solid-state reference electrode[16] was used. All potentials are reported relative to the Ag/AgCl (3 M NaCl) reference electrode. The working electrodes used included the following: 3-mm glassy carbon (macro-GCE) (BAS), 10-μm glassy carbon (GC-UME) (Cypress Systems, Lawrence, KN), 1.6-mm platinum (macro-Pt) (BAS), and an iridium ultramicroelectrode array (Ir-UMEA) consisting of 564 individual interconnected UMEs with a radius of 6 μm.

In situ observations were performed with a Metaval-H (Jenoptika Jena, GmbH, Germany) inverted polarizing microscope equipped with a videoimaging system. For these experiments a CH Instruments model 830 potentiostat (CH Instruments, Cordova, TN) was interfaced with a Toshiba Satellite T2130CT laptop computer. The electrochemical cell was constructed with a microscope slide to allow for optical viewing. Surface morphologies were recorded and evaluated with a Nanoscope-E atomic force microscope (Digital Instruments, Santa Barbara, CA).

Experimental Conditions. For ex situ mercury film formation with the macro-GCE, GC-UME, and macro-Pt electrode, the mercury was deposited from a separate deposition solution of 8 mM Hg^{2+} and 0.1 M HNO_3 with an applied potential of −0.4 V for 120 s. In all solutions, the counterion for Hg^{2+} was NO_3^-, which has no effect since it is already in abundance due to the supporting electrolyte. For the Ir-UMEA, the reduction charge was monitored and stopped when ∼20 mC had been accumulated. After the mercury film was formed, the electrode was immediately rinsed and transferred to a 0.02 M acetate buffer (pH 4.5) containing 100 ppb Cd^{2+} and Pb^{2+}. SWASV was performed using an initial potential of −1.0 V, final potential of −0.1 V, deposition time (t_d) of 120 s for the macro-GCE and macro-Pt electrode, 180 s for the GC-UME and the Ir-UMEA, frequency (f) 60 Hz for the macro-GCE and macro-Pt electrode, 120 Hz for the GC-UME and 180 Hz for the Ir-UMEA, pulse amplitude (E_{sw}) of 25 mV, and a step height (ΔE_s) of 2 mV. After the analysis, the mercury was stripped using LSV (−0.3 to 0.3 V) in 1 M KSCN at a scan rate (ν) of 10 mV/s.

In situ mercury film formation was carried out in a solution containing 0.8 mM Hg^{2+}, 0.01 M HNO_3, and 100 ppb Cd^{2+} and Pb^{2+}. The SWASV analysis was performed with an initial potential −1.0 V, final potential 0.5 V, $t_d = 120$ s for the macro-GCE, macro-Pt and Ir-UMEA, $t_d = 180$ s for the GC-UME, $f = 60$ Hz for the macro-GCE and macro-Pt, $f = 180$ Hz for the GC-UME and the Ir-UMEA, $E_{sw} = 25$ mV, and $\Delta E_s = 2$ mV. A condition step was added for the macro-Pt electrode (−0.4 V for 120 s) and the Ir-UMEA (−0.3 V for 120 s) but was eliminated after the second run. All stripping peak currents reported are the average of three scans.

Reagents. All solutions were prepared with 18 MΩ·cm deionized water from a Barnstead Nanopure system (Barnstead Co., Dubuque, IA). The acetate buffer solutions were prepared with 99.99+% sodium acetate (Fluka) and glacial acetic acid (Fisher Scientific). Metal solutions were prepared with 99.999+% $Cd(NO_3)_2$ (Aldrich), $Pb(NO_3)_2$ (Aldrich), and $Hg(NO_3)_2$ (Johnson

(16) Nolan, M.; Tan, S.; Kounaves, S. *Anal. Chem.* **1997**, *69*, 1244−1247.

Matthey). All other solutions were prepared with ACS grade reagents.

RESULTS AND DISCUSSION

Ex situ Mercury Film Formation. Since perchloric acid is a widely used electrolyte for mercury deposition, its stability is critical to mercury film formation. The effect of $HClO_4$ dissociation was investigated by the formation of mercury films on a macro-GCE over a period of 9 days. The solution used for mercury film formation consisted of 8 mM Hg^{2+} and 0.1 M $HClO_4$. For the first 3 days, the stripping peaks for Cd^{2+} and Pb^{2+} were of comparable height, but a decrease in both signals was observed on the fourth and eighth day. The oxidation charge and percent efficiency ($Q_{ox}/Q_{red} \times 100$) followed the same trend while the reduction charge remained relatively constant over the 9 days. The excess Hg^{2+} ions react with the mercury film, forming soluble Hg_2^{2+} and thus partially dissolving the mercury film. This reaction is also an indication of the increased Cl^- concentration attributable most likely to the dissociation of the ClO_4^- ion. This accounts for the decrease of the Cd^{2+} and Pb^{2+} stripping peaks, oxidation charge, and percent efficiency.

The influence of Cl^- in the mercury deposition solution was investigated by ex situ mercury film formation on a macro-GCE in a solution containing 8 mM Hg^{2+} and 0.1 M HNO_3 with varying Cl^- concentrations (0.0001−4 M). In the Cl^- concentration range of 0.0001−0.01 M, the signals for Cd^{2+} and Pb^{2+} were lower than those obtained when no Cl^- was present in the mercury deposition solution. The SWASV signals for the mercury film formed in the 0.1 and 1 M Cl^- solutions were comparable to those with no Cl^- present. The signals for Cd^{2+} and Pb^{2+} decreased slightly in the 4 M Cl^- deposition solution. From these results, it is recommended that chloride ions be eliminated from the mercury deposition solution by using a nitric acid medium instead of perchloric and a reference electrode, which does not leak Cl^-. Comparable results were obtained when the deposition solution contained 1 M Cl^-.

The influence of Cl^- on mercury film formation was also investigated using a GC-UME. The Cd^{2+} and Pb^{2+} stripping peak signals decreased slightly when 0.0001 and 0.001 M Cl^- were added to the deposition solution. The oxidation charge and percent efficiency were also lower in this range. For 0.01 and 1 M Cl^-, the stripping peak, oxidation charge, and percent efficiency increased. When 0.1 or 4 M Cl^- was present, the signals decreased compared to those obtained when no Cl^- was present. The percent efficiency of the GC-UME was never greater than 60%, and the best results were obtained with 1 M Cl^- present in the mercury deposition solution. The inconsistency of the UME could be due to the disturbance of the mercury film when the electrode was transferred between solutions.

A platinum electrode was also used to study the influence of chloride ions on the mercury deposition solution. The surface of the platinum electrode was dramatically affected by the increase in Cl^- concentration. The percent efficiency and the oxidation charge for mercury decreased with increasing Cl^- concentration. Optical investigation of the platinum electrode after the oxidation of mercury revealed that a film still remained on the surface. These accumulations are most likely a Pt−Hg amalgam which were not removed during the oxidation step. It appears that Cl^- enhances the formation of the amalgam. The Cd^{2+} and Pb^{2+} stripping signals were not affected by the amalgam formation at Cl^- concentrations below 0.001 M; however, at higher concentrations the signal decreased. Formation of an amalgam decreased the Cd^{2+} stripping signal by 1 order of magnitude and the Pb^{2+} signal by about half. Thus, mercury film formation on platinum should also be performed with no Cl^- present in the deposition solution.

Table 1. Formation Constants and Redox Potentials for Various Hg^{2+} Reactions[21]

$Hg^{2+} + nCl^- \leftrightarrows HgCl_n^{2-n}$	Log $\beta_{1-4} = 6.74, 13.22, 14.07, 15.07$
$Hg^{2+} + nSCN^- \leftrightarrows Hg(SCN)_n^{2-n}$	Log $\beta_{2,4} = 17.47, 21.23$
$Hg^{2+} + 2e^- \leftrightarrows Hg$	$E° = 0.853$ V
$2Hg^{2+} + 2e^- \leftrightarrows Hg_2^{2+}$	$E° = 0.911$ V
$Hg_2Cl_2 + 2e^- \leftrightarrows 2Hg + 2Cl^-$	$E° = 0.268$ V
$Hg_2Cl_2 \leftrightarrows Hg_2^{2+} + 2Cl^-$	$pK_{sp} = 17.88$

Ex situ mercury film formation was also carried out using an Ir-UMEA. The highest stripping peak currents for Cd^{2+} and Pb^{2+} were obtained with deposition solutions containing 0.01 and 1 M Cl^-, while the lowest peaks were obtained for 0.0001 and 0.001 M Cl^-. Peaks for mercury films formed without Cl^-, or with 0.1 and 4 M Cl^-, measured between the high and low values. The percent efficiency of the mercury deposition varied from 85 to 95%; however, no trend was seen between the percent efficiency and the stripping peak height. The Ir-UMEA gave responses similar to the macro-GC, in that the best responses were obtained with a mercury film deposited from either a solution containing 1 M Cl^- or when no Cl^- was present.

Overall, for ex situ mercury film formation, the best signals were obtained with glassy carbon or iridium substrates with either 1 M Cl^- or no Cl^- present in the deposition solution. In contrast, for the macro-Pt electrode the deposition efficiency of the mercury film decreased with increasing Cl^- concentration. Even though the electrodes were briefly at open circuit when they were removed from the plating solution and rinsed, for most mercury films, no distortions in the sequential anodic scans were observed. However, when the mercury film was formed on the macro-GCE in 0.1 M Cl^-, a cathodic peak only occurred on the first anodic scan. Thus, this scan was not used.

In Situ Mercury Film Formation. In situ formation of mercury films has many advantages over ex situ formation. However, the presence of chloride ions in the solution results in the formation of calomel on the mercury surface. Calomel is formed under open circuit conditions by the following reaction[15,17]

$$Hg^0 + Hg^{2+} + 2\,Cl^- \rightarrow Hg_2Cl_2(s)$$

One method of avoiding calomel interference is to complex the Hg^{2+} ions so they do not react with the mercury film. This is typically accomplished either by the addition of KSCN[10] or by having a Cl^- concentration greater than 3.5 M.[15] The cumulative formation constants for mercury−chloride and mercury−thiocyanate complexes and the redox potentials for various mercury reactions are tabulated in Table 1. Equilibrium calculations clearly show that calomel will not form at KSCN concentrations above 0.002 M. At this concentration, the Hg^{2+} is strongly complexed with the SCN^- as indicated by the formation constant.

(17) Jagner, D. *Anal. Chem.* **1978**, *50*, 1924−1929.

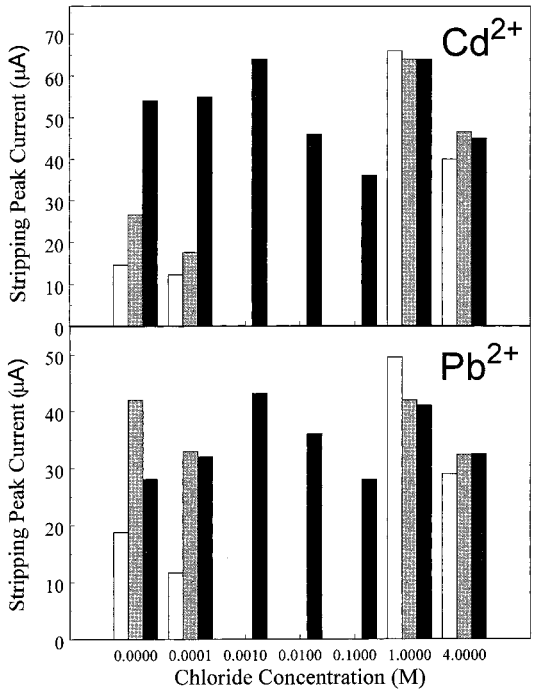

Figure 2. SWASV peak currents using a macro-GCE for 100 ppb Cd^{2+} and Pb^{2+}, in 0.8 mM Hg^{2+} and 0.01 M HNO_3 (white) with the addition of either 0.1 M KNO_3 (gray) or 0.1 M KSCN (black) at varying Cl^- concentrations.

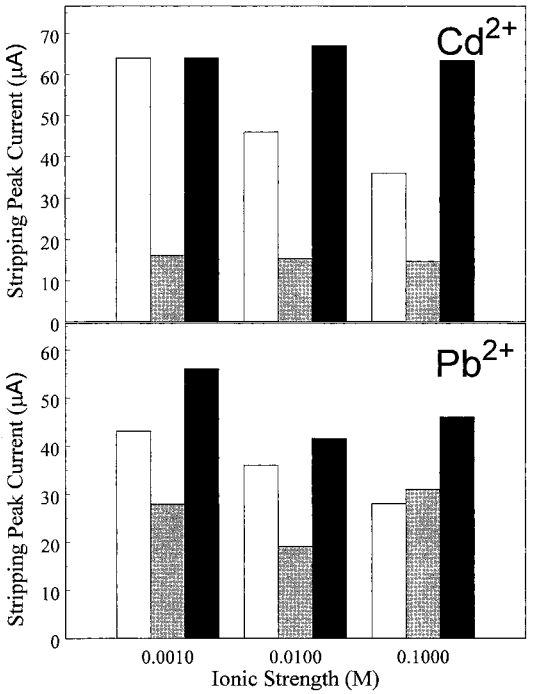

Figure 3. SWASV peak currents using a macro-GCE for 100 ppb Cd^{2+} and Pb^{2+}, in 0.8 mM Hg^{2+} and 0.01 M HNO_3 with 0.1 M KSCN and ionic strength varied by the addition of NaCl (white), 0.1 M KSCN with the ionic strength varied by the addition of KNO_3 (black), or 0.1 M KNO_3 with the ionic strength varied by the addition of KNO_3 (gray).

The formation of calomel on the GC electrodes was extensively investigated by varying the Cl^- concentration and monitoring the SWASV response for 100 ppb Cd^{2+} and Pb^{2+}. The in situ deposition solution consisted of 0.8 mM Hg^{2+} and 0.01 M HNO_3. The influence of the SCN^- was examined by addition of 0.1 M KSCN to the solution. The effect of ionic strength increase, due to the addition of the KSCN, was investigated by addition of 0.1 M KNO_3. The results for the three solutions using a macro-GCE are presented in Figure 2 for Cd^{2+} and Pb^{2+}. Calomel formation, detectable by the appearance of a cathodic peak between −0.6 and −0.3 V, was observed in the Cl^- concentration range of 0.001−0.1 M for the solutions that did not contain KSCN. Above and below this range, and also in solution containing KSCN, no cathodic peak was observed. However, in 0.0001 M Cl^-, if the final potential was set at 0 V so that the mercury film remained on the electrode, a cathodic peak appeared in the ensuing anodic scan. Furthermore, when the chloride concentration was greater than 0.001 M, a gray film remained on the electrode surface (vide infra) even when the potential was scanned to 0.5 V.

The results from the macro-GCE (Figure 2) also demonstrate that, in the lower range of Cl^- (without the addition of KSCN), a decrease of the Cd^{2+} and Pb^{2+} signals occurred when the Cl^- concentration was increased from 0 to 0.0001 M, indicating that the Hg^{2+} in solution was dissolving the mercury film. The decrease was not observed in the KSCN-containing solution because the Hg^{2+} ions were complexed. The ionic strength of the solution had a pronounced effect on the heights of the stripping peaks at low Cl^- concentrations. In this range, the peak heights for both the Cd^{2+} and Pb^{2+} were increased by addition of 0.1 M KNO_3 or KSCN to the solution. In comparing the two 0.1 M solutions, the ionic strength influenced the peaks for Pb^{2+}, while on the other hand, the Cd^{2+} peaks were drastically effected by the presence of the SCN^- ions. Above the calomel formation range (1 and 4 M), the presence of NO_3^- and SCN^- had no influence on either the Cd^{2+} or Pb^{2+} stripping peak heights.

In the calomel region (0.001−0.1 M Cl^-), the addition of SCN^- eliminated the calomel interference; however, the signal for both metals decreased with increasing Cl^- concentration. The influence of having both Cl^- and SCN^- present in solution was further examined by the addition of NO_3^- instead of Cl^-. The resulting stripping peak currents for 100 ppb Cd^{2+} and Pb^{2+} are shown in Figure 3. An increase in the stripping peak heights was observed on addition of SCN^- to either the Cl^-- or the NO_3^--containing solutions. In the SCN^- solutions, when the ionic strength was altered by the addition of NO_3^-, no decrease was observed for the Cd^{2+} peaks while the Pb^{2+} responses fluctuated with varying ionic strength. In the 0.001 M NO_3^- and SCN^- solution, the Cd^{2+} remained unchanged whereas the Pb^{2+} stripping peak was higher compared to the 0.001 M Cl^- solution. Thus, the decrease of the metal stripping peak height in the Cl^--containing solution must be due to the increase of the Cl^- concentration. The decrease may be due to the competition between the Cl^- and SCN^- ions for the complexation of Hg^{2+} ions in solution. Thus, when either Cl^- or SCN^- ions were in abundance, compared to the other anion, this effect was not observed (i.e., at low and high chloride concentrations).

The results presented above differ from those reported by Jagner et al.,[15] which showed cathodic peaks in the concentration range of 0.001 to ∼2 M Cl^-. In this study, however, no cathodic peaks were obtained at Cl^- concentrations greater than ∼0.5 M. At Cl^- concentrations greater than ∼0.2 M,[18] the prevailing inorganic species was $HgCl_4^{2-}$. Since in this case the Hg^{2+} is fully coordinated as $HgCl_4^{2-}$, it does not react with the mercury film

to form calomel on its surface. The less coordinated species ($HgCl^+$, $HgCl_2$, $HgCl_3^-$), which are the prevailing species below ~0.2 M, do react to form calomel on the mercury film.

The regions above and below the calomel-forming range were examined to determine the influence of the ionic strength and the presence of the Cl^- ions. The ionic strength of the solution was kept constant by the addition of NO_3^-. No decrease in peak height was observed when the NO_3^- concentration was increased from 0 to 0.0001 M, indicating that the decrease seen with Cl^- was due to the formation of Hg_2^{2+} ions. At high ionic strengths (1 and 4 M), the presence of Cl^- ions dramatically increased the Cd^{2+} peak. The Pb^{2+} peak was instead more influenced by the ionic strength. In fact, in the 4 M solution, the increase in the Pb^{2+} stripping peak was entirely due to ionic strength.

In situ visual observations of the macro-GCE surface were performed in the various regions of calomel formation in order to determine any effects on surface morphology. With no and 0.0001 M Cl^- ions in the mercury deposition solution, the electrode turned dark red, green, and then gray during the reduction of the Hg^{2+} onto the GC surface. After anodically stripping the mercury film (final potential of 0.5 V), the electrode appeared unchanged from its original morphology with no film remaining on the surface. During the deposition of mercury from a 1 M Cl^- solution, the electrode again turned red, green, and then gray. However, after the anodic scan, a gray film still remained on the electrode surface. In the 0.1 M Cl^- solution, the electrode again turned red, green, and then gray during the deposition, but a lighter gray-white film remained on the GC surface. After the second scan, the electrode surface appeared rough and nonuniform. During the anodic scan, no change in the electrode surface was observed. The above results demonstrated that the electrode surface was indeed altered in the calomel region, but the remnant of the mercury film does not correlate with the cathodic peak.

In situ mercury deposition was also performed on a GCE−UME. The stripping peak heights for 100 ppb Cd^{2+} and Pb^{2+} were recorded for a solution containing 0.8 mM Hg^{2+} and 0.01 M HNO_3 and also with either 0.1 M KNO_3 or 0.1 M KSCN. Similar results, as shown in Figure 4, were obtained with the micro-GCE as with the macro-GCE. The calomel formation region was the same (0.001−0.1 M chloride). As before, a decrease in signal was observed when the chloride concentration was increased from 0 to 0.0001 M without the addition of KSCN. The presence of SCN^- increased the stripping peak for Cd^{2+} and also increased the Pb^{2+} peak in the 0.0001 M Cl^-. The ionic strength of the solution had no effect on the peak for Cd^{2+} or Pb^{2+} because of the properties of microelectrodes. At high concentrations of Cl^-, the presence of NO_3^- and SCN^- had little influence on the stripping peaks of either metal. In the KSCN solutions, the Pb^{2+} peaks decreased with increasing Cl^- concentration in the calomel formation region, but the Cd^{2+} peaks fluctuated and showed no trend.

A Pt macroelectrode was also used for "in situ" mercury deposition; however, the mercury deposition was performed as a conditioning step before the deposition of the analyte metals. No cathodic peak was observed during the anodic scan when the conditioning step was performed. However, when the conditioning

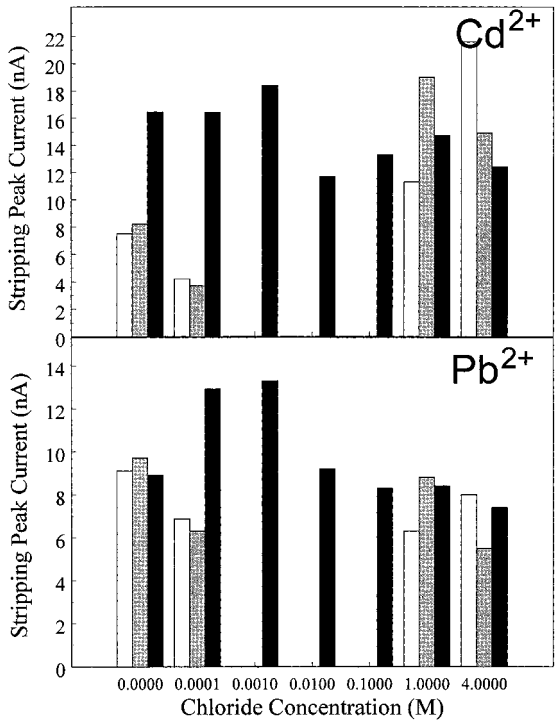

Figure 4. SWASV peak current using a GC-UME for 100 ppb Cd^{2+} and Pb^{2+} in a solution containing 0.8 mM Hg^{2+} and 0.01 M HNO_3 (white) with the addition of either 0.1 M KNO_3 (gray) or 0.1 M KSCN (black).

was eliminated, a cathodic peak was observed during the anodic scan. The efficiency of the mercury film formation decreased with no Cd^{2+} peak obtained for the 100 ppb solution and a 2-fold decrease for the Pb^{2+} peak. The calomel region was determined to be the same as for the macro-GCE. For all solutions, a thin opaque film remained on the platinum surface that could not be electrochemically removed. This film may be the result of either inadequate removal of the mercury or the formation of a platinum−mercury amalgam. From the results obtained in this study, it would appear that "in situ" mercury deposition on a platinum surface is not a viable procedure for performing ASV analyses.

Finally, in situ mercury deposition was performed on an array of iridium ultramicroelectrodes (Ir-UMEAs) in a solution containing 0.8 mM Hg^{2+} and 0.01 M HNO_3 with various Cl^- concentrations. Monitoring the stripping peak current for 100 ppb Cd^{2+} and Pb^{2+} assessed the efficiency of the mercury film formation. Again, initial mercury deposition was performed as a conditioning step but was eliminated after two scans. Even though the potential was scanned to +0.4 V, the mercury was not efficiently removed from the Ir-UMEA surfaces and thus the stripping peak height increased with every run. To eliminate this effect, the first three runs in each solution were averaged and the mercury was removed after each solution by LSV in 0.1 M KSCN.

The results for the Ir-UMEA show trends similar to those observed with both GC macro- and microelectrodes (Figure 5). The calomel interference occurred in the region of 0.001−0.1 M Cl^-. Although if open circuit conditions were allowed in the 0.0001 M Cl^- solution for more than 5 min, a cathodic peak was observed in the subsequent anodic scan. The presence of SCN^- increased the peak height for Cd^{2+} while the increase for the Pb^{2+} stripping

(18) Moore, J. W.; Ramamoorthy, S. *Heavy Metals in Natural Waters*; Springer: New York, 1984.

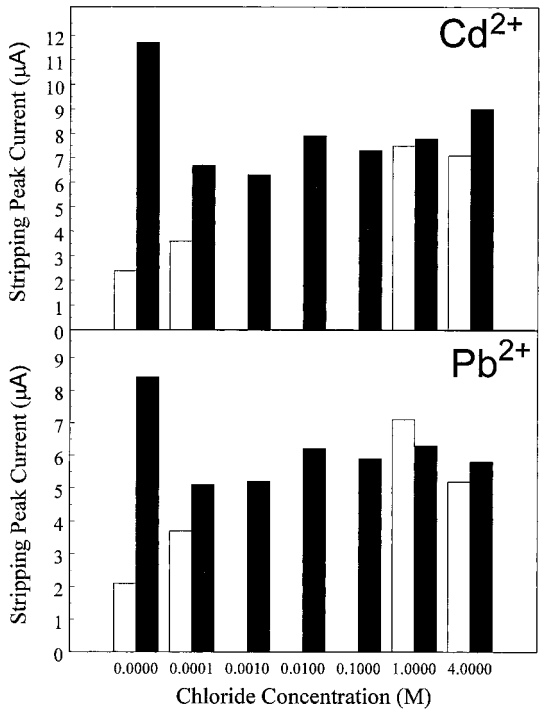

Figure 5. SWASV peak current using an Ir-UMEA for 100 ppb Cd^{2+} and Pb^{2+} in 0.8 mM Hg^{2+} and 0.01 M HNO_3 (white) plus the addition of 0.1 M KSCN (black).

peak was most likely due to a combination of both the SCN^- and the increase in the ionic strength. At high concentrations of Cl^- (1 and 4 M), the SCN^- had little effect on the peak height. However, two major differences between the Ir-UMEA and GC electrodes were apparent: (1) there was no decrease in stripping peak height when the Cl^- concentration was increased from 0 to 0.0001 M, and (2) in the calomel region the stripping peak current was more reproducible when SCN^- was in the solution. These differences are also probably due to the incomplete removal of the mercury from the electrode surface.

Since including a conditioning step before the deposition of the analyte metals eliminated the cathodic peak on both the Ir-UMEA and Pt macroelectrode, the same conditioning step was also applied to the GC electrodes. This step was performed in a solution containing 0.8 mM Hg^{2+}, 0.1 M NaCl, and 0.01 M HNO_3 at a potential of −0.3 V and at times from 30 to 240 s. However, the cathodic peak still occurred during the anodic scans. This cathodic peak is an indication that calomel has formed on the electrode surface; what is not clear is whether calomel can form without the accompanying cathodic peak response. To further resolve this anomaly, in situ mercury deposition was performed on an Ir-UMEA in a solution containing 0.8 mM Hg^{2+}, 0.01 M HNO_3, and varying Cl^- concentrations. No conditioning step was applied during the second SWASV scan. After the end of the second scan, the mercury was removed by an anodic linear scan in 0.1 M KSCN. For solutions containing 10^{-4} M > $[Cl^-]$ > 1 M (i.e., above and below the calomel region), no accumulations appeared on the iridium surface. For solutions lying within the calomel region, when the conditioning step was eliminated and the cathodic peak occurred, no accumulations were seen on the Ir-UMEA surfaces after the removal of the mercury film. However, when the condition time was applied and then the mercury film was removed, accumulations remained on the electrode surface. Using AFM, the images of the accumulations were similar to those that were previously identified as being calomel.[19] Thus, applying a conditioning step to either the macro-Pt or the Ir-UMEA eliminated the cathodic peak but did not eliminate the formation of the calomel.

Different Voltammetries. Square wave anodic stripping voltammetry was performed in all of the above experiments. Two other voltammetric techniques, LSV and DPV, were also investigated to determine whether the cathodic peak was in some way related to the technique itself. In both of these voltammetric techniques, even though its shape was slightly different, the cathodic peak was still present. With either SWV or DPV, the cathodic peak appeared as a large sharp spike while in LSV it appeared as a dip (Figure 1). These differences are most likely due to the time scale and pulsed potential perturbation between the LSV and SWV or DPV techniques. Jagner et al.[15] noted that once the phase change from calomel to mercury had begun, it only took a fraction of a second to occur. Thus, with SWV the large pulse amplitudes (E_{sw} = 25 mV) at f = 60 Hz cause rapid reorientation, whereas with LSV the phase change occurs gradually as the potential is scanned at a constant rate of 500 mV/s.

Substrate Dependence. A HMDE was used to confirm that calomel would also form even though the electrode was composed entirely of pure mercury and, if at such an electrode, it would not form at high Cl^- concentrations. Previous work[20] showed that abnormal current response occurred with a DME in a chloride-containing solution. In a solution containing 0.8 mM Hg^{2+}, 0.01 M HNO_3, and 0.1 M NaCl, the cathodic peak not only appeared but totally masked the Pb^{2+} stripping peak. However, when the experiment was run in a solution containing 1 M Cl^-, no cathodic peak appeared. Therefore, calomel formation is independent of whether the mercury is coated on a substrate or in pure form.

CONCLUSION

For ex situ mercury film formation on iridium and glassy carbon substrates, the highest efficiency was obtained when no Cl^- or 1 M Cl^- was present in the deposition solution. The platinum surface was drastically influenced by the presence of the Cl^- ions; thus, during ex situ mercury film formation, the best results were obtained with no Cl^- ions present. The formation of calomel during in situ mercury deposition was found to occur in the Cl^- concentration range of 0.001−0.5 M and to be independent of the substrate material used. During in situ mercury film formation, the Pb^{2+} stripping peak current was increased by the increased ionic strength of the solution while the Cd^{2+} peak current was dramatically increased by the presence of SCN^- or Cl^- ions. Although conditioning of the Ir-UMEA and Pt macroelectrode did eliminate the cathodic peak, calomel still remained on the electrode surface after the mercury film was removed. However, when the cathodic peak occurred, after the removal of the mercury film no calomel remained on the electrode surface. For in situ mercury film formation the calomel interference can be easily avoided. If the Cl^- concentration is greater than 0.01 M, the best results are obtained by adjusting it to 1 M. If the Cl^- concentration is less than 0.01 M, the addition of SCN^- ions is

(19) Nolan, M. A.; Kounaves, S. P. *J. Electroanal. Chem.* **1998**, *453*, 39−48.
(20) Kolthoff, I. M.; Miller, C. S. *J. Am. Chem. Soc.* **1941**, *63*, 1405−1411.
(21) *Lange's Handbook of Chemistry*, 4th ed.; McGraw-Hill: New York, 1992.

preferable. Although analysis can be preformed when no Cl^- is present in the solution, extra precautions are needed to ensure unintentional contamination of the sample by any extraneous sources.

ACKNOWLEDGMENT

This work was supported in part by grants from the Environmental Protection Agency through the Northeast Hazardous Substance Research Center at NJIT and the National Science Foundation (CHE-9256871). The authors also thank Jim Doyle at the IBM Watson Research Center for the fabrication of the iridium UMEAs and Rosemary Feeney for her assistance.

Received for review July 27, 1998. Accepted January 6, 1999.

AC9808270